ISSN: 0067-2904

Effect of Aluminum Dust Particles on Plasma Parameters at Different Gas Pressure with Different Dust Contents

Shahad Emaduldeen Abdulghani, Qusay Abbas Adnan , Omar Abdulsada Ali*
Department of Physics, College of Science, University of Baghdad, Baghdad, Iraq

Received: 26/11/2023 Accepted: 5/1/2025 Published: 15/2/2025

Abstract

In this work, the effect of aluminum (Al) dust particles on the DC discharge plasma properties in argon was investigated. A magnetron is placed behind the cathode at different pressures and with varying amounts of Al. The plasma temperature (T_e) and density (n_e) were calculated using the Boltzmann equation and Stark broadening phenomena, which are considered the most important plasma variables through which the other plasma parameters were calculated. The measurements showed that the emission intensity decreases with increasing pressure from 0.06 to 0.4 Torr, and it slightly decreases with the addition of the NPs. The calculations showed that the n_e increased and T_e decreased with pressure. Both T_e and n_e were reduced by increasing the content of aluminum dust.

Keywords: Dust plasma, spectroscopy, electron temperature, electron density,

تأثير جسيمات غبار الالمنيوم على خصائص البلازما عند ضغوط غاز مختلفة وبكميات غبار مختلفة

شهد عماد الدين عبد الغني, قصي عدنان عباس, عمر عبد السادة علي*
قسم الفيزياء, كلية العلوم, جامعة بغداد,بغداد, العراق

الخلاصة

تم في هذا العمل دراسة تأثيرجسيمات غبار الألمنيوم (Al) على خواص بلازما التفريغ المستمر في الأرجون بوجود مغنطرون خلف الكاثود عند ضغوط مختلفة وبكميات مختلفة من Al. تم حساب درجة حرارة البلازما (T_e) والكثافة (n_e) باستخدام معادلة بولتزمان وظاهرة توسع ستارك، والتي تعتبر من أهم متغيرات البلازما التي تم من خلالها حساب معاملات البلازما الأخرى. أظهرت القياسات أن شدة الانبعاث تتناقص مع زيادة الضغط من 0.06 إلى 0.4 Torr وانخفضت بشكل طفيف مع إضافة NPs. وأظهرت الحسابات أن ne تزداد مباشرة مع الضغط ، بينما تتناقص Te مع الضغط. قل كل من T_eو n_e مع زيادة محتوى غبار الألومنيوم.

1. Introduction

Dusty plasma is a plasma that contains a micron or nanosized particles suspended in it. Dust particles are charged, with charges up to several hundred or thousand elementary charges, and thus dramatically change the behavior of the plasma [1,2]. Dust particles can aggregate to form larger particles, forming "grain plasma". Dusty plasma is also known as complex plasma due

*Email: omar.ab@sc.uobaghdad.edu.iq

to the additional challenge that lies in diagnosing plasma phenomena in the presence of this charged dust.
Dusty plasma has unique phenomena due to the effects of charged particles on the plasma's charge balance. It can exist in different states, ranging from weakly bonded to liquid-like and crystalline, depending on the strength of the electrostatic coupling between the grains. These plasmas are useful for studying self-organization and phase transitions in fundamental physics [3]. The dust has a negative or positive charge, causing the electric field distortion. The negative charge is the dominant one. Some authors suggest that electrically charged dust grains may also create a large magnetic distortion [4]

In dusty plasma, thousands of negatively charged electrons are trapped by the electric field, which is created due to the large surface negative charge [5,6]. This results in the formation of a bulk of dust plasma. Dust particles can grow by sputtered particles or reactive gases [7]. Dusty plasma is observed in various phenomena occurring in the Earth's atmosphere [8], in addition to the cosmic plasma surrounding many planets, such as Saturn's rings and comets [9,10]. Dusty plasma can be studied in the laboratory in cases that need to study the effect of dust on plasma, which is essential in different applications [3]. In many applications, it is necessary to control the properties of dust plasma [11]. Plasma is used in the microelectronic industry using complicated materials [4]. Because of the extensive use of plasma dust systems and the ease with which parameters may be controlled, dusty plasma is a research subject with both physical and technological benefits [12]. Studies of dusty plasma dynamics are of interest when the dust component is magnetized in magnetic fields. A magnetic field also causes a rotation of the dusty plasma in a plane horizontal to the field lines due to Lorentz force and obtaining a stable discharge [13,14].

In this study, the effect of aluminum nano-powder dusted in DC discharges magnetron plasma on its parameters at different vacuum pressures and dust contents is investigated.

1.1 Theoretical Description of Dusty Plasma Parameters

One of the most important ways to obtain plasma parameters is through the use of plasma diagnostics. Emission spectroscopy is a highly significant method for diagnosing plasma and providing its parameters [15]. The Boltzmann plot is used to determine plasma temperature (T_e) by measuring the slope of the linear relation [16]:

$$Ln\left(\frac{I_{ji}\lambda_{ji}}{h\,c\,g_j A_{ji}}\right) = \left(-\frac{E_j}{k_B T_e}\right) + Constant \quad (1)$$

where I_{ji}, is the intensity, A_{ji} is the probability of transition from *i* to *j*, g_j is a statistical weight of upper *j* level, *h* is Planck's constant, and λ_{ji} is the wavelength.

The Stark broadening phenomena is used in the calculation of plasma density (n_e) using line broadening $\Delta\lambda$ [17,18]:

$$n_e(cm^{-3}) = \left[\frac{\Delta\lambda}{2\omega_s}\right] N_r \quad (2)$$

where ω_s is the electron-impact value and *Nr* is the reference density.
Many parameters describe plasma behavior, including plasma frequency, which is calculated according to plasma density as [19,20]:

$$\omega_{pe} = \sqrt{\frac{n_e\, e^2}{m_e\, \varepsilon_0}} \quad (3)$$

where $\varepsilon_0$is the free space permittivity, m_e is the electron mass.

Debye's length is calculated depending on the electron density and temperature [19,20]:

$$\lambda_D = \sqrt{\frac{\varepsilon_0 \, k_B \, T_e}{e^2 \, n_e}} \quad (4)$$

where k_B is Boltzmann's constant.

2. Experimental setup:

The experiments were carried out with a DC magnetron discharge system with a duster, as shown in Figure 1. The plasma discharge in argon was operated in DC voltage under vacuum with pressures ranging from 0.06 to 0.4 Torr. Two circular plane aluminum electrodes with a diameter of 6 cm were utilized. The electrodes were isolated by Teflon to prevent any electrical sparks and fixed at a right angle with each other. The normal glow discharge was produced by 3 kV DC power supply with the assistance of a circular magnetron behind the cathode. Different weights of aluminum as dust were introduced into the plasma discharge to investigate the impact of this dust on plasma properties. An optical emission spectrometer device was used to diagnose the plasma parameters at different working pressures and weights of aluminum dust.

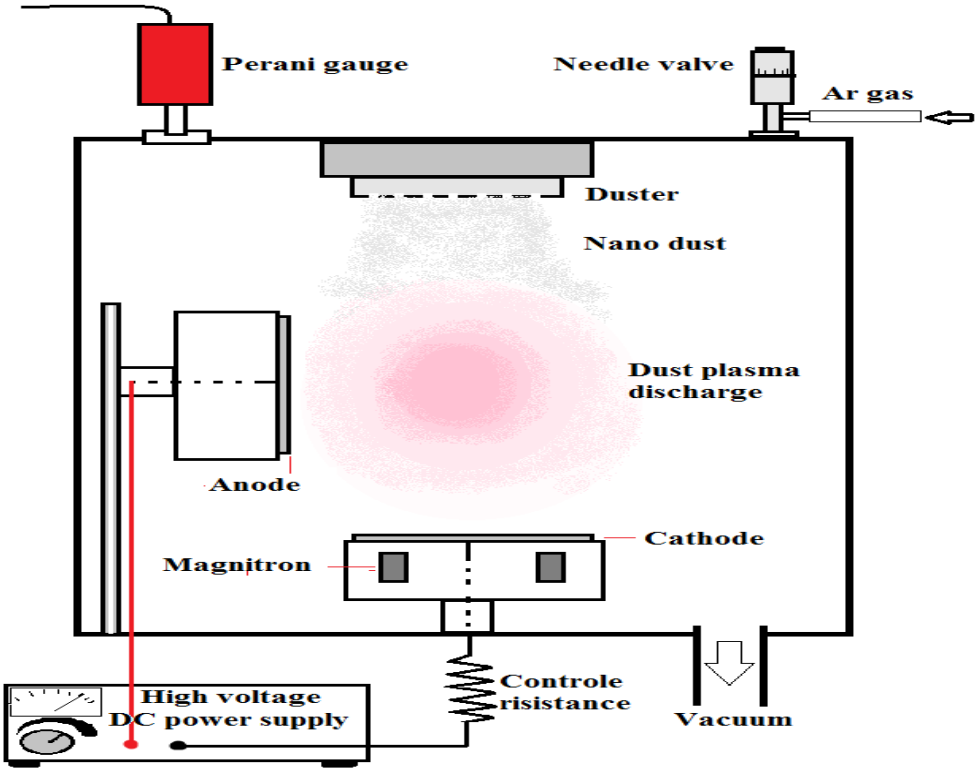

Figure 1: Illustration of DC magnetron discharge dust plasma system

3. Results and Discussions

3.1 Emission Spectra of Dusty Plasma

The plasma emission spectra from the DC magnetron discharge system at different gas pressures with different contents of dust are shown in Figure 2. Many peaks corresponding to atomic and ionic argon emission lines appeared with different intensities according to the transition probability. The *Hα* peak at 656.7 nm is caused by residual hydrogen atoms and can provide information about the statistical weight of upper levels and plasma temperature. Small peaks corresponding to aluminum emission appeared. In general, the spectral lines intensities decreased with increasing the working pressure from 0.06 to 0.4 Torr due to the reduction of

the excitation collision cross-section as a result of reducing electron energy by different collision types with atoms.

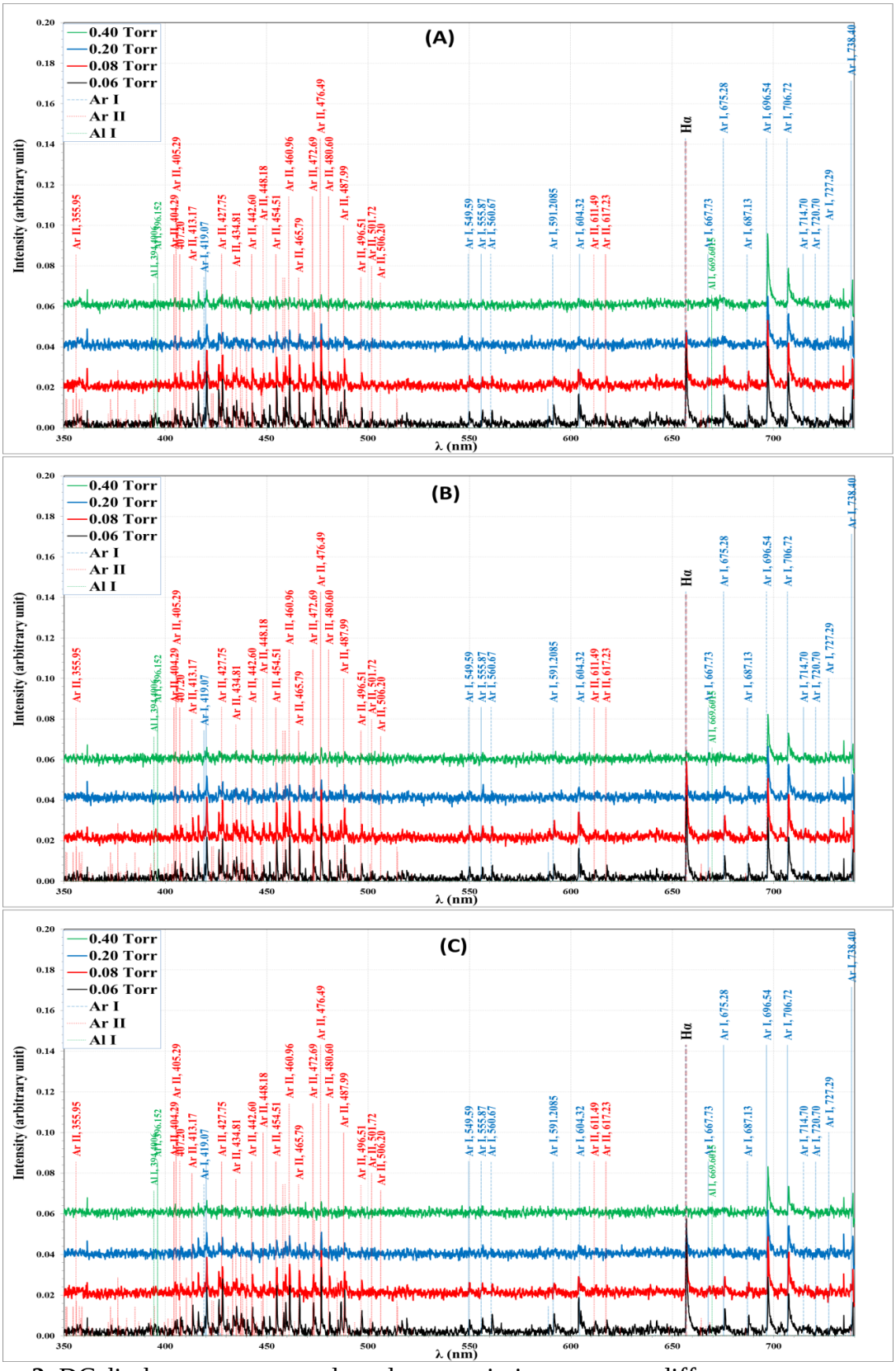

Figure 2: DC discharge magnetron dust plasma emission spectra at different gas pressure using (a)100mg Al_2O_3, (b) 150mg Al_2O_3 and (c) 200mg Al_2O_3.

Figure 3 shows a comparison between plasma emission spectra at different aluminum dust weights for DC discharge magnetron plasma at 0.06 Torr gas pressure. The dust slightly reduced the emission intensity, especially for ionic transition, indicating the reduction of the ionization ratio as a result of altering the charged dust of the plasma. The mean free path of elastic collisions being reduced, causing reduced excitation collisions.

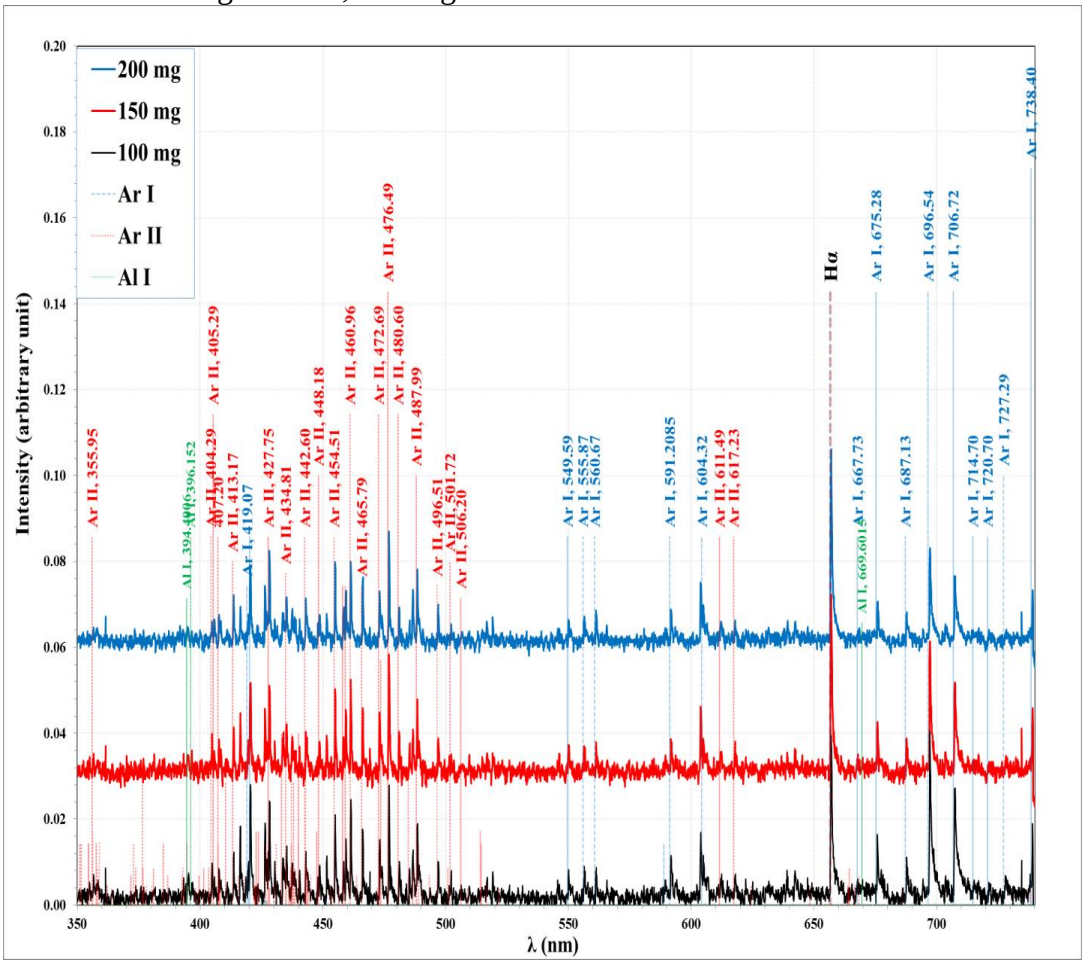

Figure 3: DC discharge magnetron plasma emission spectra in Ar at 0.06 Torr pressure with different Al_2O_3 dust contents.

3.2 Influence of Al dust concentrations on the dusty plasma parameters

Plasma temperature (T_e) was measured using Boltzmann plot for the different conditions, as shown in Figure 4. The lines parameters for the ionic argon species were used from the national institute of standard and technology (NIST) [19]. The best linear fit for the relation between $Ln(I_{ij}\lambda_{ij}/ hc\ g_j\ A_{ij})$ versus the upper-level energies (E_j) is shown in Figure 4. The T_e is equal to the inverse of the slope.

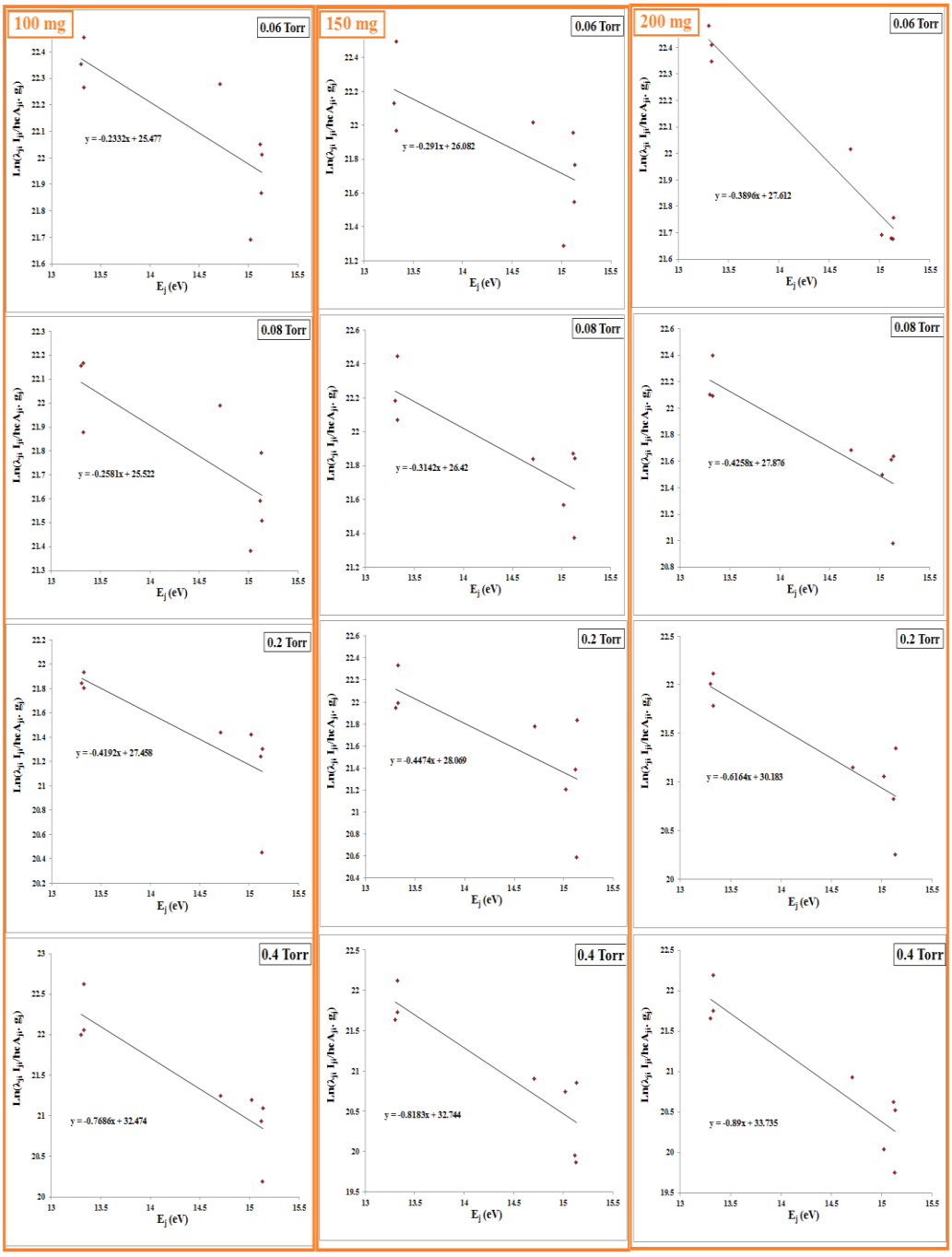

Figure 3: Boltzmann plots using the observed ArlI lines at different gas pressures and dust contents.

Figure 4 illustrates the variation of T_e with the working gas pressures for the three weights of aluminum dust. The electron temperature decreased with the increase of the working pressure from 0.06 to 0.4 Torr as a result of increasing electron-atom collisions. In these collisions, a specific amount of the electron energy is transferred, causing reduced kinetic energy of the electrons. In addition, an increase in dust contents decreased T_e and was severely affected at lower pressures than at higher pressures. The dust contents are affected at low pressure as a result of the increased collisions with these particles compared to the low density of the gas atoms. On the other hand, its effect is low at high pressure due to the high density of the gas atoms [22,23].

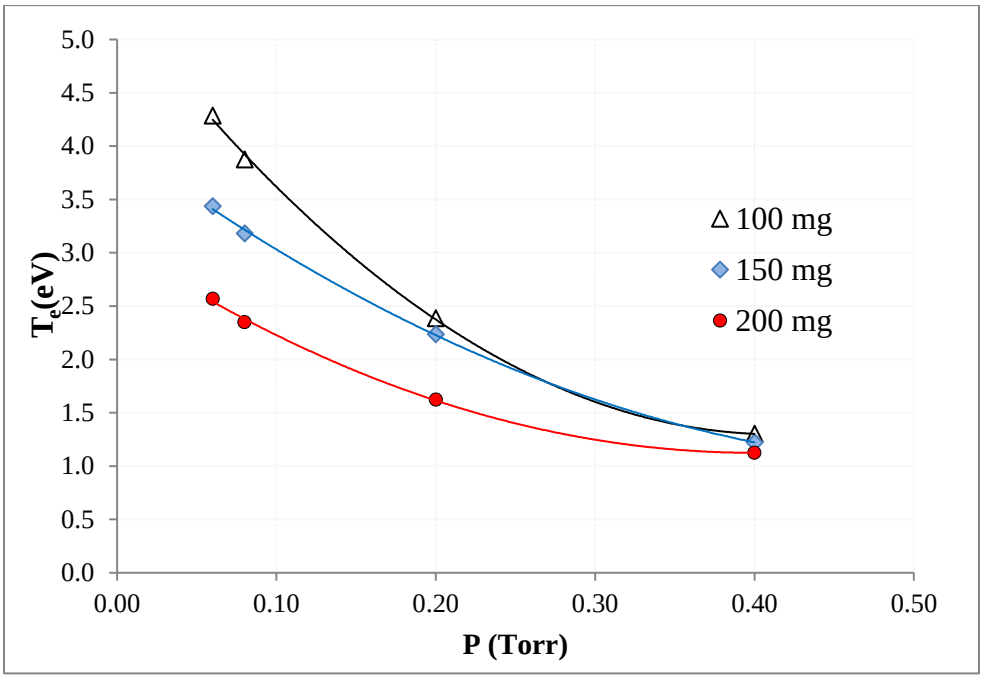

Figure 4: The change of T_e with working pressure at different dust content.

The electron density (n_e) was determined using Stark's broadening phenomena. The full width at half-maximum values ($\Delta\lambda$) For the *Ar II* line at 476.49 nm are shown in Figure 5. The Lorentzian Fitting was used to measure the different Al contents and pressures, as seen in Figure 4. Although the broadening slightly varies for different cases.

The n_e value was determined by utilizing the parameters of the (*Ar II* 476.49 nm) emission line, using ω_s = 0.0384 nm and Nr =1.0×10^{17} cm^{-3} in equation 2 [24,25].

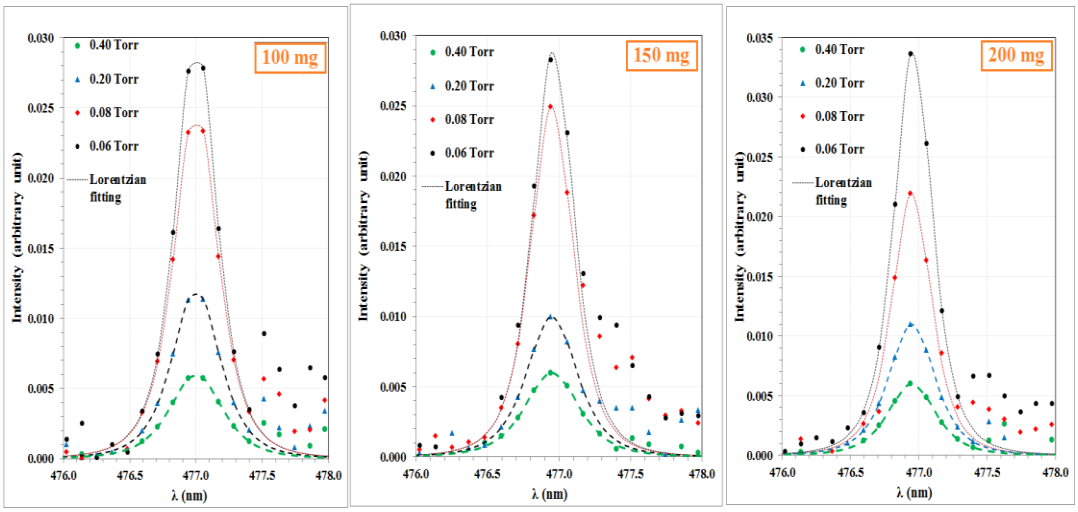

Figure 5: Lorentzian fitting for the Ar II line at 476.49 nm at various gas pressures and dust contents.

Figure 6 illustrates the change of the electron density with pressure at different dust contents. n_e increased with the working pressure. Where the electron number density increased from 4.82×10^{17} to 6.12 ×10^{17} cm^{-3}, from 4.42×10^{17} to 5.86 ×10^{17} cm^{-3} and from 4.3×10^{17} to 5.3 ×10^{17} cm^{-3} at 100, 150, and 200 mg Al NPs dust contents, respectively. The density Increases with pressure at this range of gas pressure due to growing electrons-atoms ionization collision

probability, which in turn increases the ionizing reactions that supply the plasma with additional charged particles. The reduction of n_e with increasing dust as a result reduce the electron kinetic energy, due to the turbulence caused by the increasing space charge carried by the dust particles, which causes the reduction of the ionization collision probability.

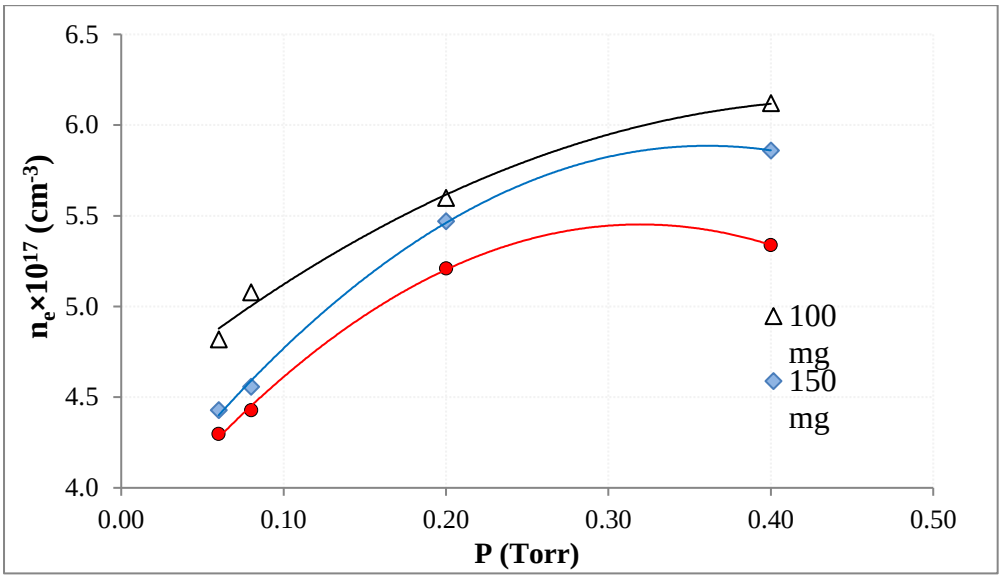

Figure 6: The change of n_e with working pressure at different dust contents.

Table 7 illustrates the change of plasma parameters for the dust plasma discharge with magnetron with the Al dust contents at different gas pressures. It is clear that the plasma frequency (*fp*) increases with increasing the working pressure and decreases with increasing the dust contents as a direct relation with plasma density, which is highly affected by space charge that causes plasma complexity. The Debye length (λ_D) reduced with increasing the working pressure as a result of increasing the electron density, which increases the plasma shielding effect. Furthermore, increasing the dust contents caused more reduction in λ_D.

Table 7: Plasma parameters for the DC discharge magnetron plasma at different pressures and dust contents.

Dust weight (mg)	P (Torr)	T_e (eV)	λ (nm)Δ	$n_e \times 10^{17}$ (cm^{-3})	$f_p \times 10^{12}$ (Hz)	$\lambda_D \times 10^{-6}$ (cm)
100	**0.06**	4.287	0.370	4.818	6.233	2.217
	0.08	3.874	0.390	5.078	6.399	2.052
	0.20	2.385	0.430	5.599	6.719	1.534
	0.40	1.301	0.470	6.120	7.025	1.083
150	**0.06**	3.436	0.340	4.427	5.975	2.070
	0.08	3.183	0.350	4.557	6.062	1.963
	0.20	2.235	0.420	5.469	6.641	1.502
	0.40	1.222	0.450	5.859	6.874	1.073
200	**0.06**	2.567	0.330	4.297	5.886	1.816
	0.08	2.349	0.340	4.427	5.975	1.711
	0.20	1.622	0.400	5.208	6.481	1.311
	0.40	1.124	0.410	5.339	6.561	1.078

4. Conclusions

In this work, the effect of aluminum dust in DC discharge plasma magnetron at different contents of aluminum was studied. It was observed that the intensity of the spectral lines decreased with increasing pressure and the dust content in the plasma. The space charge carried by the dust particles disturbed the electric field, causing changes in plasma parameters. An increase in aluminum dust content led to a decrease in both plasma temperature and density, which in turn changed other plasma parameters. Therefore, the presence of dust inside the plasma in the deposition systems must be considered, as it greatly affects the properties of the deposited films.

References:

[1] L. G. D'yachkov, O. F. Petrof. and V. E. Fortov, "Dusty Plasma Structures in Magnetic DC Discharges," *Contrib. Plasma Phys,* vol. 49, no. 3, pp. 134-147, 2009.

[2] A. K. Bard and Q. A. Abbas, "Influence of Cylindrical Electrode Configuration on Plasma Parameters in a Sputtering System," *Iraqi Journal of Science,* vol. 63, no. 8, pp. 3412-3423, 2022.

[3] G. E. Morfil. and A. V. Ivlev, "Complex plasmas: An interdisciplinary research field," *Reviews of Modern Physics,* vol. 81, no. 4, p. 1353–1404, 2009.

[4] M. W. Morooka, J. E. Wahlund, D. J. Andrews, A. M. Persoon, S. Y. Ye, W. S. Kurth, D. A. Gurnett, and W. M. Farrell, "The Dusty Plasma Disk Around the Janus/Epimetheus Ring," *J. Geophys. Res. Sp. Phys.,* vol. 123, no. 6, p. 4668–4678, 2018.

[5] T. F. Toussaint, "The charge distribution of dust particles in plasma afterglow," *Faculteit Technische Natuurkunde,* 2017.

[6] Q. A. Abbas, R. R. Abdula and B. T. Chied, "The axial profile of plasma characteristics of cylindrical magnetron sputtering device," *Iraqi Journal of Physics,* vol. 8, no. 11, p. 41 – 47, 2010.

[7] V. Vekselman, Y. Raitses, and M. N. Shneider, "Growth of in dynamic plasma," *Physical Review E,* vol. 99, p. 063205, 2019.

[8] N. Borisov and H. Krüger, "Formation of the Thebe Extension in the Ring System of Jupiter," *J. Geophys. Res. Sp. Phys.,* vol. 126, p. e2021JA029654, 2021.

[9] R. Merlino, "Dusty plasmas: from Saturn's rings to semiconductor processing devices," *Adv. Phys. X,* vol. 6, no. 1, 2021.

[10] A. K. Bard and Q. A. Abbas, "Influence of cylindrical magnetron sputtering configurations on plasma characteristics," *Optik,* vol. 272, p. 170346, 2023.

[11] E. S. Dzlieva, L. G. D'yachkov, L. A. Novikov, S. I. Pavlov, and V. Y. Karasev,"Dusty Plasma in Inhomogeneous Magnetic Fields in a Stratified Glow Discharge," *Molecules,* vol. 26, p. 3788, 2021.

[12] B. Lindstrom, P. Bélanger, A. Gorzawski, J. Kral, A. Lechner, B. Salvachua, R. Schmidt, A. Siemko, M. Vaananen, D. Valuch, C. Wiesner, D. Wollmann, and C. Zamantzas, "Dynamics of the interaction of dust particles with the LHC beam," *Phys. Rev. Accel. Beams,* vol. 23, no. 12, p. 124501, 2020.

[13] E. S. Dzlieva, V. Y. Karasev, and S. I. Pavlov, "Dynamics of Plasma−Dust Structures Formed in a Trap Created in the Narrowing of a Current Channel in a Magnetic Field," *Dusty Plasma,* vol. 42, p. 142–149, 2016.

[14] Z. M. Abbas, Q. A. Abbas, "Aluminum-doped ZnO nano-laminar structures by pulsed laser ablation for gas sensing application," *Journal of Optics,* vol. 53, no. 1, pp. 544-557, 2023.

[15] M. Zhukov, Plasma Diagnostics, vol. 22, Mosco: Lightning Source UK Ltd, 2005.

[16] S. S. Hamed, "Spectroscopic Determination of Excitation Premixed Laminar Flame," *Egypt. J. Solids,* vol. 28, no. 2, p. 349–357, 2005.

[17] N. M. Shaikh, S. Hafeez, B. Rashid, and M. A. Baig, "Spectroscopic studies of laser induced aluminum plasma using fundamental, second and third harmonics of a Nd: YAG laser," *Eur. Phys. Journal D,* vol. 44, p. 371–379, 2007.

[18] S. E. Abdulghani and Q. A. Abbas, "Effect of Fe2O3 Nanoparticles Dust on the D.C Plasma Characteristics with Mirror Magnetron," *Iraqi Journal of Science,* vol. 64, no. 5, pp. 2297-2305, 2023.

[19] C. Fallon, "Optical Diagnostics of Colliding Laser Produced Plasmas: Towards Next Generation Plasma Light Sources," Ph.D. thesis, Dublin City University, 2013.

[20] S. E. Abdulghani and Q. A. Abbas, "Influence of Fe2O3 Dust Particles on the Plasma Characteristics of D.C Sputtering System," *Iraqi Journal of Science,* vol. 63, no. 7, pp. 2945-2954, 2022.

[21] " NIST Atomic Spectra Database," [Online]. Available: http://kinetics.nist.gov/index.php.

[22] A. Ahmed, M. O. Salman, M. Alwazzan, and A. Meri, "Blushers Component Analysis for Unbranded Cosmetic Brands: Elements Concentration Levels and its Effect on Human Body," *Jour Adv Res. Dyn. Control Syst.,* vol. 2, pp. 1-8, 2019.

[23] O. A. Ali, S. S. Al-Awadi, "Synthesis and Characterization of Cu2FeSnSe4Nanofilms," *Iraqi Journal of Science,* vol. 62, no. 6, pp. 1873-1878, 2021.

[24] N. KonjeviÄ and W. L. Wiese, "Experimental Stark widths and shifts for spectral lines of neutral and ionized atoms," *J. Phys. Chem. Ref. Data,* vol. 19, no. 6, p. 1307–1385, 1990.

[25] O. A. Ali, "Estimated the nanoparticles size of CdS from UV–Vis spectrum absorption by effective mass approximation model (EMA) using capping and complex agent," *Journal of Optics,* vol. 53, no. 2, pp. 1551 - 1556, 2024.